ELSEVIER

Carbohydrate Research 337 (2002) 2211–2222

CARBOHYDRATE RESEARCH

www.elsevier.com/locate/carres

Morphology of Western larch arabinogalactan

Rengaswami Chandrasekaran,* Srinivas Janaswamy

Whistler Center for Carbohydrate Research, Food Science Building, Purdue University, West Lafayette, IN 47907-1160, USA

Received 4 April 2002; accepted 6 May 2002

Dedicated to Professor Derek Horton on the occasion of his 70th birthday

Abstract

A molecular modeling study has revealed that (1→3)-β-D-galactan can not only adopt a triple helical structure similar to that of the corresponding glucan but can also accommodate a highly flexible β-D-Gal-(1→6)-β-D-Gal disaccharide moiety as a side group 6-linked to every galactosyl unit in the main chain. The resulting triple helix, applicable to Western larch arabinogalactan, can assume quite different morphologies since the side group has access to several allowed conformational states. Some of the preferred modes of association between these helices have been visualized using preliminary X-ray fiber diffraction data.

Keywords: Arabinogalactan; Plant polysaccharide; X-ray diffraction; Molecular modeling

1. Introduction

Structural studies to date have revealed that polysaccharides can adopt a host of molecular structures of varying complexity.[1,2] For example, cellulose and mannan chains are simple 2-fold ribbon-like structures that tend to assemble in sheets through lateral association. The amylose molecule is a left-handed, 6-fold double helix in which the two coaxially interwound chains of the same polarity are connected by hydrogen bonds between their hydroxyl groups. Unlike the monosaccharide repeat for the above, ι-carrageenan and gellan are composed of disaccharide and tetrasaccharide repeats, respectively. They exist as 3-fold double helices in which the two chains also intertwine coaxially in a parallel fashion as in amylose. While the former requires its sulfate groups, gellan uses its carboxylate groups for helix–helix aggregation via cations and water molecules. In contrast, the (1→3)-linked polymers such as β-glucan (or curdlan) and β-xylan, having a

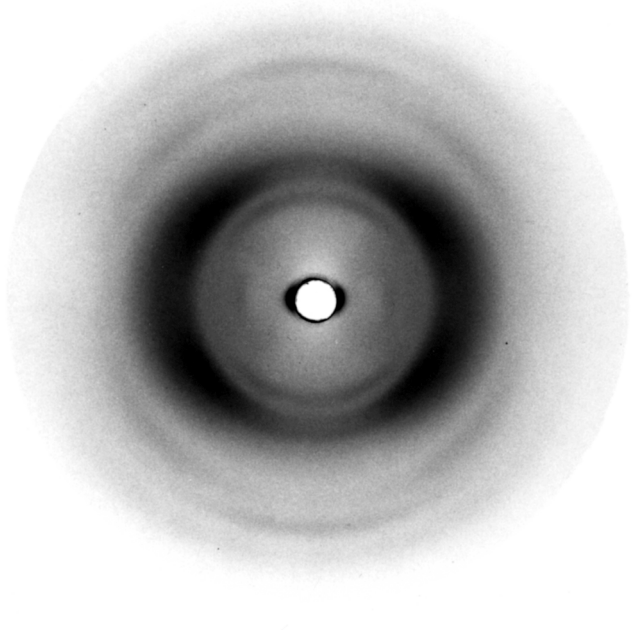

Fig. 1. X-ray diffraction pattern from a slightly oriented fiber of arabinogalactan kept at 31% r.h. using Cu K_α radiation of wavelength 1.5418 Å.

* Corresponding author. Tel.: (765) 494-4923; fax: (765) 494-7953

E-mail address: chandra@purdue.edu (R. Chandrasekaran).

0008-6215/02/$ - see front matter
PII: S0008-6215(02)00223-9

monosaccharide repeat similar to that in cellulose or mannan, favor triple-helical structures composed of three coaxially interwound polysaccharide chains, related by 3-fold rotational symmetry around the molecular axis such that every repeat in one chain forms O-2H···O-2 hydrogen bonds with the other two to provide structural stability.

The morphologies observed for linear polymers are apparently quite robust as evident from X-ray studies of related branched polysaccharides. This is illustrated vividly by the galactomannan structure,[3] which resembles those of cellulose and mannan; by welan[4] and RMDP17[5] that have a gellan backbone sequence, monosaccharide and disaccharide side groups, respectively, in every repeat unit, and yet retain a gellan-like double-helix; and by scleroglucan[6] having the curdlan backbone,[7] and a (1→6)-linked glucosyl unit side group in every third repeat in the main chain that still maintains the triple-helical form. The side groups describe the periphery and increase helix stability through hydrogen bonds with the main chain.

Certain linear polymers having the same linkage type are also able to adopt extremely similar molecular morphologies. For example, cellulose, mannan and glucomannan (Konjac mannan) are all (1→4)-linked polymers that are composed of glucose, mannose and glucose/mannose, respectively. Their molecular structures are virtually identical because the canonical 2-fold ribbon structure of pitch about 10.4 Å is fully compatible with either equatorial (in glucose) or axial orientation (in mannose) of the hydroxyl group at position 2. It is thus reasonable to expect structural similarity between (1→3)-β-D-glucan and (1→3)-β-D-galactan since galactose is the C-4-epimer of glucose. In other words, the reported curdlan triple-helical structure[7] may be viable for the (1→3)-galactan so long as switch-

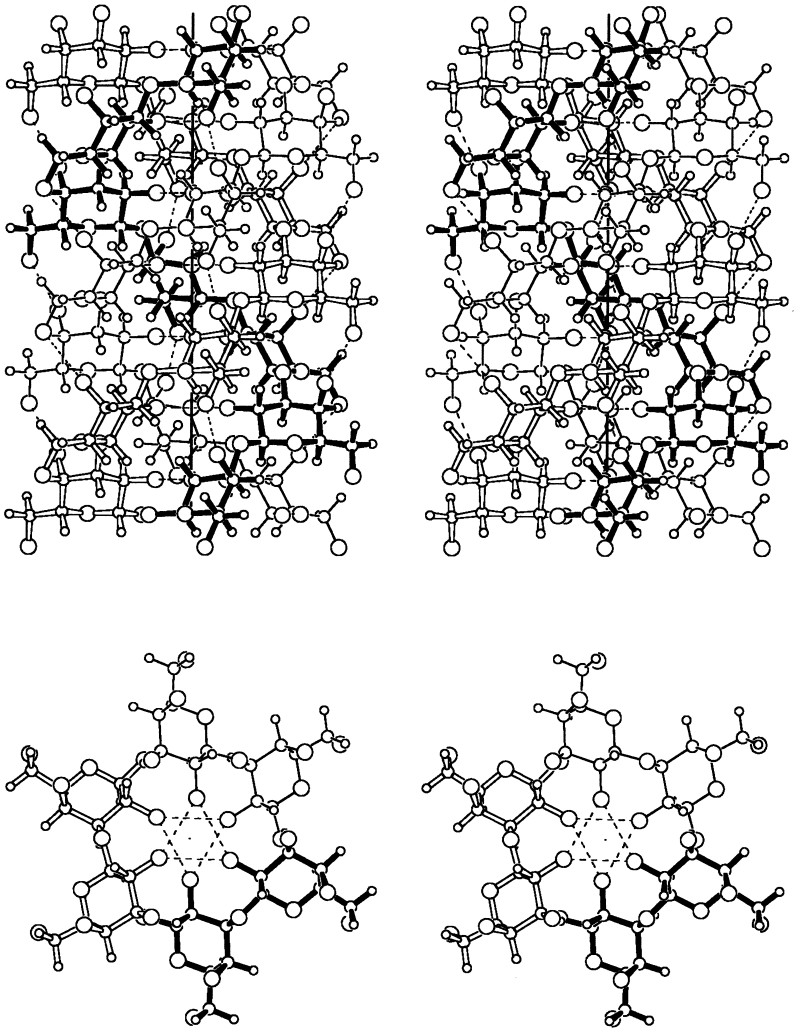

Fig. 2. Stereo drawing of two mutually normal views of the (1→3)-β-D-galactan triple helix. In the side view (top) the vertical line is the helix axis. The axial view (bottom) clearly shows the formation of O-2H···O-2 hydrogen bonds (dashed lines) between neighboring 3-fold related chains.

Table 1
Statistics for the triple helical models of arabinogalactan in different conformational domains of χ (°)

Set	χ_A	χ_B	χ_C	*E*	*J*	*C*	Ω
1	60	60	60	3	35	22	25
2	60	180	180/−60	1	28	11	12
3	60	−60	180/−60	1	21	9	10
4	180	60	60	4	33	32	36
5	180	180	60/180/−60	1	24	12	13
6	180	−60	60	2	31	12	14
7	−60	60	60	5	47	40	45
8	−60	180	60/180/−60	1	15	9	10
9	−60	−60	60/180/−60	1	14	9	10

E, *C* and Ω refer to the conformation angles varied, contacts applied and the global term in Eq. (1). The variables contributing to *E* are (ϕ_B, ψ_B) and (ϕ_C, ψ_C). One or more angles listed under χ_C represent the preferred domains.

ing the equatorial hydroxyl group to axial orientation at atom C-4 does not introduce steric anomalies. To our knowledge, this has not been verified so far, and we have now examined the hypothesis.

An extension of this modeling analysis is to investigate structural homology, if any, between scleroglucan and arabinogalactan. The term arabinogalactan covers several branched polysaccharides[8–12] that contain both arabinosyl and galactosyl units and are gaining attention as potential drug carriers. We have focused on a simpler system, Western larch arabinogalactan (*Larix occidentalis*), a water-soluble polysaccharide. It has a maximum molecular weight of about 37 000 Da. A third of the molecule consists of a (1→3)-β-D-galactopyranan main chain, and the rest corresponds to side groups (1→6)-linked to every galactosyl unit, whose size ranges from a monosaccharide to oligosaccharide. The side group distribution is not uniform. Often, the side group is the disaccharide β-D-Gal*p*-(1→6)-β-D-Gal*p* or β-L-Ara*p*-(1→3)-α-L-Ara*f*. Less frequent is a single β-D-Gal*p* or α-L-Ara*f* or a dimer β-L-Ara*p*-(1→3)-α-L-Ara*f*.[8] For the sake of simplicity, we have approximated the repeating unit of arabinogalactan to the trisaccharide shown below:

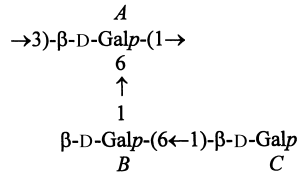

The important result of this study is that the (1→3)-β-D-galactan can also adopt a curdlan-like triple helical structure to which the disaccharide *CB* can be conveniently attached as a side group so as to provide the first prototype molecular model representing larch arabinogalactan. This finding is supported by preliminary X-ray fiber diffraction data obtained from this material.

2. Experimental and modeling details

Sample preparation.—A pure powder sample of larch arabinogalactan was provided by Larex, Inc. (St. Paul, MN). Slightly oriented fibers could be prepared using a concentrated aqueous solution (2% w/v) of the polymer.

X-ray data.—Diffraction patterns were recorded on photographic films in a pinhole camera on a microfocus X-ray generator. One of the best patterns (Fig. 1) was chosen for measuring the approximate unit cell dimensions. The two equatorial reflections correspond to *d*-spacings of 24.5 and 8.1 Å. The meridional reflections are in the form of arcs at spacings 8.9 and 2.95 Å on the 2nd and 6th layer lines, respectively. The other reflections are broad at 4.4 Å on the 4th and 2.5 Å on the 7th layer lines. These spacings are roughly in agreement with a hexagonal unit cell of dimensions $a = 28.4$ and c (fiber axis) = 17.7 Å.

Modeling analysis

(a) Model building and refinement. The Linked-Atom Least-Squares (LALS) program[13] was used in generating the molecular models of galactan and arabinogalactan incorporating $^4C_1$ chair conformations for the pyranosyl rings and examining the most probable packing arrangement of the arabinogalactan helices. The

Table 2
Major conformation angles (°) for the three selected molecular structures and statistics for their final packing models

Model	χ_A	ψ_B	ϕ_B	χ_B	ψ_C	ϕ_C	χ_C	μ	*J*	*C*	Ω
1	66	166	−111	−60	−159	−85	−162	13	64	25	26
2	175	179	−107	−173	158	−78	−170	19	59	26	27
3	−66	−152	−100	−53	171	−91	−64	−1	57	24	25

In all the models, the galactan core has $\phi_A = -90°$, $\psi_A = 129°$, $\tau = 116.6°$. The first term *E* in Eq. (1) is 1 from the *I* variables listed in columns 2 through 9.

Table 3
Cartesian and cylindrical polar atomic coordinates of a trisaccharide repeat of the arabinogalactan triple helix in models **1**, **2** and **3**

	Unit	Atom	*x* (Å)	*y* (Å)	*z* (Å)	*r* (Å)	ϕ (°)
Core	*A*	C-1	3.379	1.338	0.088	3.635	21.60
		C-2	2.686	1.560	1.426	3.106	30.15
		C-3	2.395	3.038	1.636	3.869	51.75
		C-4	3.666	3.858	1.457	5.322	46.46
		C-5	4.327	3.519	0.126	5.578	39.12
		C-6	5.657	4.218	−0.061	7.057	36.71
		O-1	3.743	0.000	0.000	3.743	0.00
		O-2	1.485	0.798	1.466	1.686	28.24
		O-3	1.871	3.241	2.950	3.743	60.0
		O-4	4.589	3.579	2.508	5.820	37.95
		O-5	4.582	2.109	0.044	5.044	24.71
		H-1	2.712	1.652	−0.728	3.176	31.35
		H-2	3.331	1.194	2.238	3.538	19.72
		H-3	1.648	3.351	0.891	3.734	63.81
		H-4	3.418	4.929	1.482	5.998	55.26
		H-5	3.652	3.791	−0.699	5.264	46.07
Model **1**	*A*	O-6	6.634	3.757	0.873	7.624	29.53
		H-61	6.034	4.027	−1.076	7.254	33.72
		H-62	5.526	5.301	0.083	7.658	43.81
	B	C-1	7.952	4.108	0.614	8.951	27.32
		C-2	8.529	4.766	1.860	9.770	29.20
		C-3	10.014	5.040	1.681	11.211	26.71
		C-4	10.740	3.766	1.266	11.381	19.33
		C-5	10.053	3.141	0.056	10.532	17.35
		C-6	10.659	1.810	−0.336	10.812	9.64
		O-2	7.821	5.972	2.125	9.840	37.36
		O-3	10.563	5.529	2.906	11.922	27.63
		O-4	10.733	2.820	2.332	11.097	14.72
		O-5	8.649	2.910	0.262	9.125	18.60
		O-6	12.042	1.934	−0.665	12.196	9.12
		H-1	7.986	4.813	−0.230	9.324	31.07
		H-2	8.425	4.083	2.717	9.362	25.86
		H-3	10.154	5.810	0.909	11.699	29.78
		H-4	11.781	4.006	1.004	12.443	18.78
		H-5	10.137	3.820	−0.805	10.833	20.65
		H-61	10.130	1.410	−1.214	10.228	7.93
		H-62	10.565	1.103	0.502	10.623	5.96
	C	C-1	12.586	0.924	−1.448	12.620	4.20
		C-2	13.774	1.494	−2.211	13.855	6.19
		C-3	14.495	0.394	−2.976	14.500	1.56
		C-4	14.857	−0.750	−2.038	14.876	−2.89
		C-5	13.624	−1.209	−1.267	13.678	−5.07
		C-6	13.942	−2.270	−0.234	14.126	−9.25
		O-2	13.319	2.510	−3.097	13.554	10.67
		O-3	15.681	0.923	−3.572	15.708	3.37
		O-4	15.849	−0.332	−1.103	15.852	−1.20
		O-5	12.966	−0.138	−0.570	12.966	−0.61
		O-6	12.771	−2.969	0.185	13.112	−13.09
		H-1	11.827	0.560	−2.156	11.840	2.71
		H-2	14.495	1.923	−1.500	14.622	7.56
		H-3	13.844	0.018	−3.779	13.844	0.07
		H-4	15.249	−1.595	−2.625	15.332	−5.97
		H-5	12.887	−1.627	−1.969	12.990	−7.20
		H-61	14.646	−2.999	−0.662	14.950	−11.57
		H-62	14.396	−1.797	0.649	14.508	−7.11

Table 3 (*Continued*)

	Unit	Atom	*x* (Å)	*y* (Å)	*z* (Å)	*r* (Å)	ϕ (°)
Model **2**	*A*	O-6	6.312	3.802	−1.258	7.368	31.06
		H-61	5.496	5.305	−0.116	7.639	43.99
		H-62	6.315	3.988	0.790	7.469	32.27
	B	C-1	7.533	4.402	−1.538	8.725	30.30
		C-2	8.535	3.311	−1.891	9.155	21.20
		C-3	9.851	3.922	−2.347	10.603	21.71
		C-4	9.609	4.922	−3.469	10.796	27.13
		C-5	8.544	5.932	−3.054	10.401	34.77
		C-6	8.175	6.885	−4.170	10.688	40.10
		O-2	8.733	2.470	−0.761	9.075	15.79
		O-3	10.727	2.889	−2.802	11.110	15.08
		O-4	9.164	4.251	−4.646	10.102	24.88
		O-5	7.321	5.313	−2.619	9.045	35.97
		O-6	7.307	7.923	−3.716	10.778	47.31
		H-1	7.880	4.956	−0.654	9.309	32.17
		H-2	8.147	2.713	−2.730	8.587	18.42
		H-3	10.331	4.432	−1.498	11.242	23.22
		H-4	10.544	5.458	−3.692	11.873	27.37
		H-5	8.914	6.527	−2.206	11.048	36.21
		H-61	9.088	7.350	−4.572	11.688	38.96
		H-62	7.662	6.332	−4.971	9.940	39.57
	C	C-1	7.285	9.087	−4.473	11.647	51.28
		C-2	6.007	9.849	−4.145	11.537	58.62
		C-3	6.000	11.203	−4.839	12.708	61.83
		C-4	7.275	11.970	−4.515	14.007	58.71
		C-5	8.497	11.106	−4.808	13.984	52.58
		C-6	9.794	11.771	−4.398	15.313	50.24
		O-2	4.882	9.073	−4.539	10.303	61.72
		O-3	4.863	11.955	−4.411	12.906	67.86
		O-4	7.298	12.336	−3.137	14.333	59.39
		O-5	8.459	9.832	−4.143	12.970	49.29
		O-6	10.932	11.057	−4.880	15.548	45.33
		H-1	7.301	8.830	−5.542	11.458	50.41
		H-2	5.961	10.039	−3.062	11.675	59.30
		H-3	5.926	11.057	−5.927	12.545	61.81
		H-4	7.322	12.880	−5.130	14.816	60.38
		H-5	8.548	10.897	−5.887	13.849	51.89
		H-61	9.829	12.792	−4.808	16.132	52.46
		H-62	9.854	11.815	−3.301	15.385	50.17
Model **3**	*A*	O-6	5.501	5.632	−0.177	7.873	45.67
		H-61	6.141	3.848	−0.976	7.247	32.07
		H-62	6.304	4.012	0.805	7.473	32.48
	B	C-1	6.464	6.302	−0.921	9.028	44.28
		C-2	5.765	7.350	−1.779	9.341	51.89
		C-3	6.786	8.210	−2.507	10.652	50.42
		C-4	7.788	8.792	−1.518	11.745	48.47
		C-5	8.383	7.683	−0.658	11.371	42.50
		C-6	9.302	8.211	0.423	12.408	41.44
		O-2	4.901	6.700	−2.703	8.301	53.81
		O-3	6.117	9.269	−3.195	11.106	56.58
		O-4	7.149	9.738	−0.663	12.081	53.72
		O-5	7.385	6.886	0.003	10.097	43.00
		O-6	10.306	9.074	−0.110	13.732	41.36
		H-1	6.995	5.586	−1.565	8.951	38.61
		H-2	5.177	8.018	−1.134	9.544	57.15
		H-3	7.318	7.598	−3.250	10.550	46.08

Table 3 (*Continued*)

Unit	Atom	x (Å)	y (Å)	z (Å)	r (Å)	ϕ (°)
	H-4	8.597	9.294	−2.069	12.661	47.23
	H-5	8.963	6.997	−1.293	11.371	37.98
	H-61	9.802	7.369	0.924	12.263	36.94
	H-62	8.714	8.779	1.159	12.370	45.21
C	C-1	11.082	9.766	0.812	14.771	41.39
	C-2	12.480	9.936	0.232	15.952	38.53
	C-3	13.330	10.812	1.138	17.164	39.04
	C-4	12.618	12.128	1.422	17.501	43.87
	C-5	11.205	11.861	1.931	16.317	46.63
	C-6	10.404	13.132	2.124	16.754	51.61
	O-2	13.077	8.656	0.061	15.682	33.50
	O-3	14.589	11.071	0.512	18.314	37.19
	O-4	12.533	12.913	0.235	17.995	45.86
	O-5	10.439	11.020	1.052	15.179	46.55
	O-6	10.969	13.966	3.135	17.758	51.85
	H-1	11.134	9.194	1.750	14.439	39.55
	H-2	12.414	10.443	−0.742	16.222	40.07
	H-3	13.519	10.285	2.086	16.987	37.26
	H-4	13.175	12.689	2.186	18.292	43.92
	H-5	11.256	11.341	2.899	15.979	45.21
	H-61	9.377	12.876	2.421	15.928	53.94
	H-62	10.382	13.698	1.181	17.188	52.84

The cylindrical coordinates of the next repeat are (r, $\phi+60°$, $z+2.95$ Å). The coordinates for the second and third chains are (r, $\phi+120°$, z) and (r, $\phi-120°$, z), respectively. To place the helix in the unit cell, add μ to ϕ.

function minimized in the least-squares procedure is given by

$$\Omega = \sum_{i=1}^{I} e_i \Delta\theta_i^2 + \sum_{j=1}^{J} k_j \Delta c_j^2 + \sum_{h=1}^{H} \lambda_h G_h$$
$$= E \qquad + C \qquad + L \tag{1}$$

The term E retains the I varied conformation angles and related parameters to be in their standard or expected domains; C optimizes the model against the J non-bonded as well as hydrogen bonding interactions; and L becomes zero when the H constraints on helix symmetry are fully satisfied. The parameters e_i and k_j are the weights associated with the observations in the first two summations, respectively.

(b) (1→3)-β-D-galactan. The starting model was adapted from the triple-helix of curdlan III.[7] This consists of three identical, 6-fold, right-handed glucan helices of pitch 17.7 Å intertwined in a parallel fashion about the molecular axis. In this setup, the individual chains are related by triad symmetry about the common helix axis. The hydroxyl groups at position 4 were flipped to the axial orientation in order to obtain the galactan molecule. The two conformation angles [ϕ(O-5–C-1–O-3–C-3), ψ(C-1–O-3–C-3–C-4)] around the glycosidic bonds and the bridge bond angle τ initially set at 116.5°, were the major variables that could alter the shape of the main chain.

(c) Arabinogalactan. The side-group geometry is defined by the six major conformation angles (χ_A, ψ_B, ϕ_B) and (χ_B, ψ_C, ϕ_C), along with the terminal χ_C, where χ(C-4–C-5–C-6–O-6) refers to the C-6–O-6 bond orientation. By holding χ at 60°, 180° and −60° respectively, three sets of hard-sphere [ϕ(O-5–C-1–O-6–C-6), ψ(C-1–O-6–C-6–C-5)] maps for the Gal-(1→6)-Gal moiety were computed. The center of the allowed domain in the map was adopted as the starting point while attaching B to A and subsequently C to B. For each of the 27 distinct (χ_A, χ_B, χ_C) domains, the 4 parameters ϕ_B, ψ_B, ϕ_C and ψ_C were refined using the intrahelical interactions as observations in order to obtain proper side group attachment. Finally, the packing analysis was investigated by treating the linear galactan core as a rigid body and varying the seven conformation angles in the side group along with the orientation μ (rotation about the c-axis) of the helix so as to maximize favorable association among the helices in the hexagonal lattice.

3. Results

Galactan geometry.—The modeling calculation demonstrated that a triple helix of curdlan displaying interchain O-2H···O-2 hydrogen bonds in the interior, occurring periodically at 2.95-Å intervals along the

molecular axis, could be easily transformed into a (1→3)-galactan molecule. Switching the 4-OH group from equatorial to axial orientation encountered no steric interference. Due to this alteration, the weak O-4H···O-5 (3.2 Å) intrachain hydrogen bond present in curdlan III[7] is no longer possible in the galactan. However, a new hydrogen bond, intrachain O-4H···O-6 (2.6 Å) for *gauche plus* χ_A, or interchain O-4H···O-6 (2.7 Å) as shown in Fig. 2 for *trans*, is formed that bestows additional stability to the galactan triple helix. Its diameter (15.3 Å) is the same as in curdlan.

Arabinogalactan architecture.—While χ_A and χ_B are critical in molding the helix, χ_C is important in helix-helix association. The statistics from the modeling analysis of side group attachment to the galactan core are listed in Table 1. A survey of the data highlights that the values of *C* can be divided into two groups: 'low' 9–12 and 'high' 22–40 indicating that sets 1, 4 and 7 with gauche *plus* χ_B are not favored as they suffer from serious short contacts. In contrast, the remaining sets indicate that all the three staggered domains for χ_A and χ_C are permissible. They cannot be discriminated at

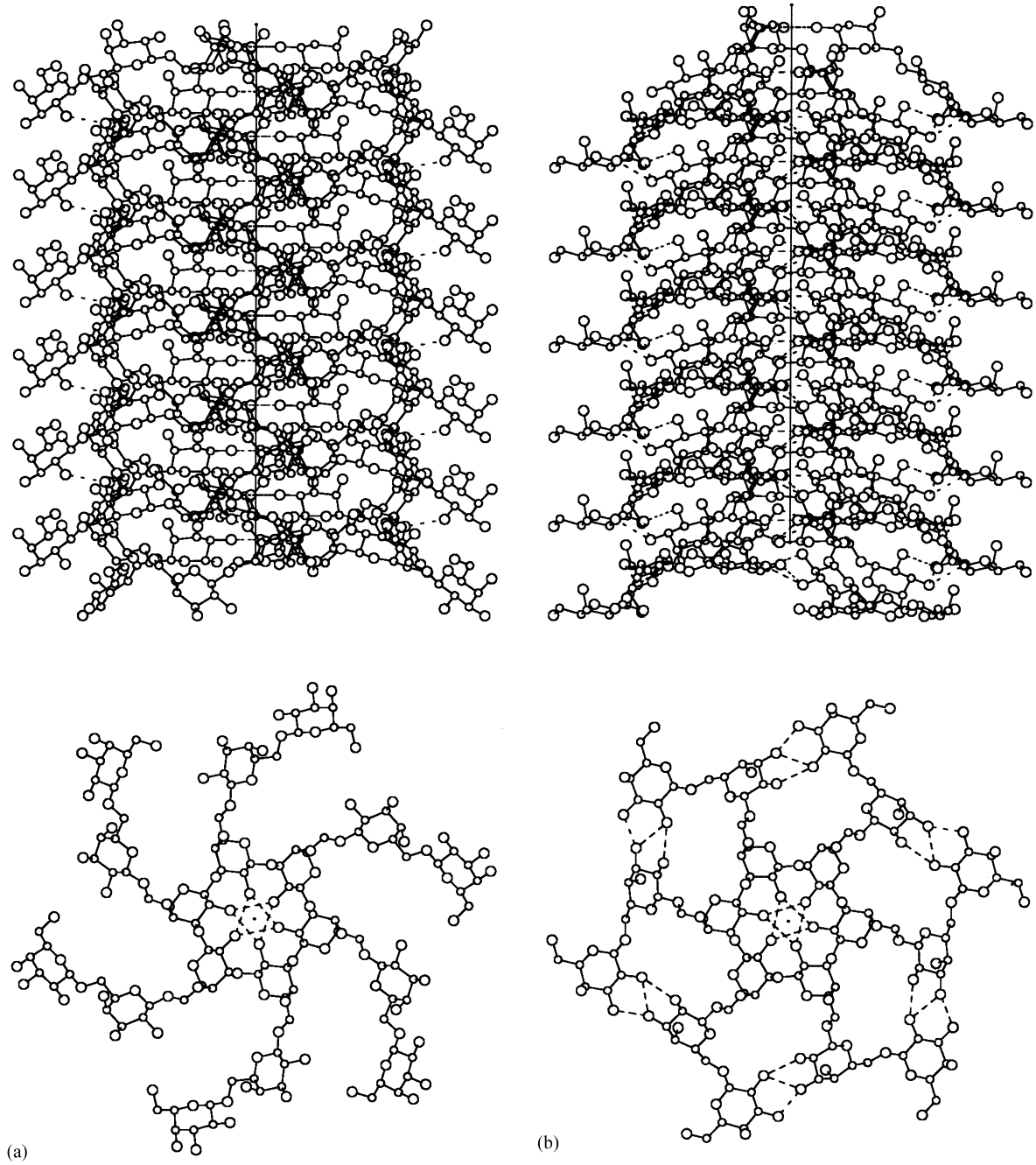

Fig. 3. Two mutually perpendicular views of two turns of the arabinogalactan triple helix in models (a) **1**, (b) **2** and (c) **3**. Their respective fingerprints, namely pinwheel, hexagon and snowflake shapes are discernible in the bottom panels.

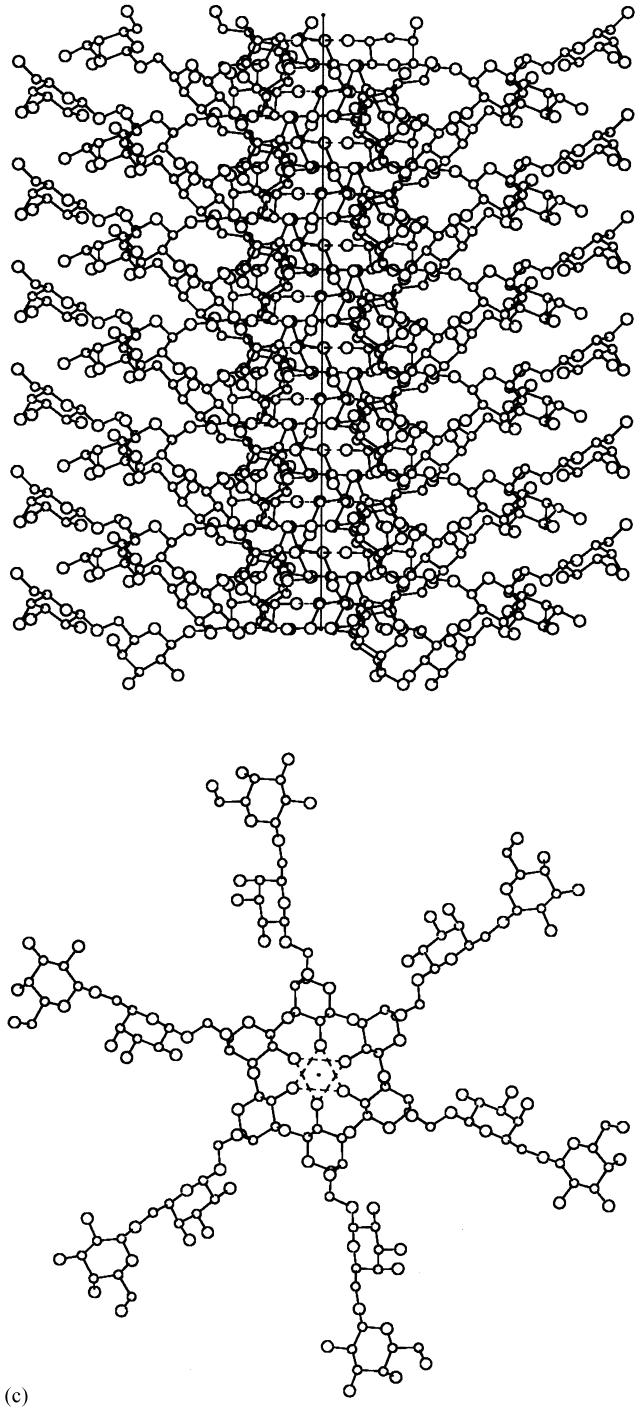

Fig. 3. (*Continued*)

99.5% confidence level based on the Hamilton's test.[14] The same conclusion is reached when Ω is surveyed as the statistic. The inference is that χ_A allows g^+, g^- and t domains, χ_B tolerates only g^- and t; but χ_C can be in any domain. Such a large conformational freedom suggests that the arabinogalactan molecule can display many distinct shapes.

Molecular packing.—In the absence of clear superiority for any particular structure, three sets having (χ_A, χ_B, χ_C) equal to (60°, −60°, 180°), (180°, 180°, 180°) and (−60°, −60°, −60°), respectively, each representing a different staggered domain for χ_A, were selected for examining the packing arrangement. The unit cell is adequate for one turn of the triple helix; positioned at

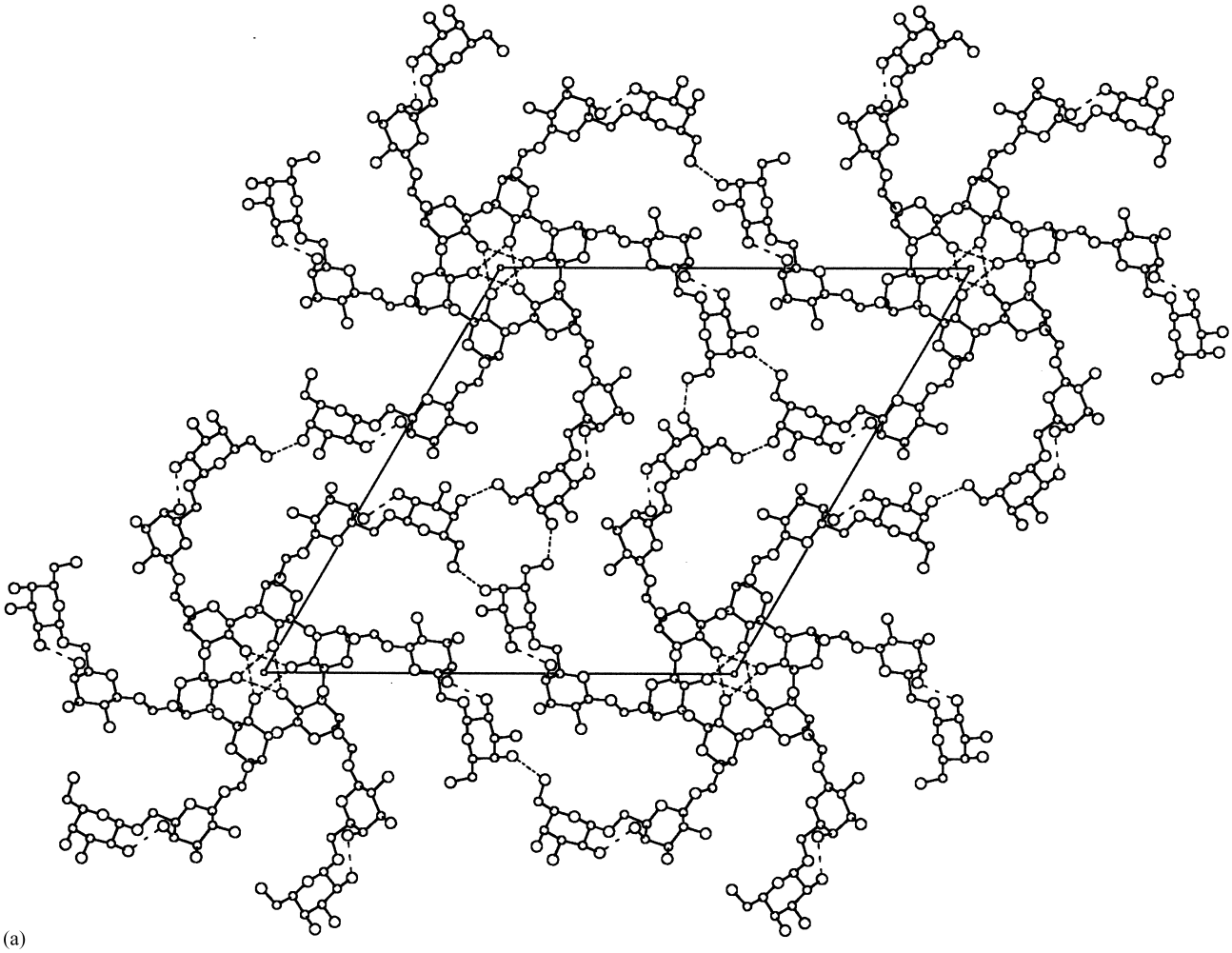

Fig. 4. Probable hexagonal packing arrangements viewed down the molecular axis in models (a) **1**, (b) **2** and (c) **3**. The helices are linked by hydrogen bonds.

the origin, its molecular axis coincides with the *c*-axis. The analysis proceeded smoothly and produced side group activated hydrogen bonds between the helices. The major conformation angles and statistics for the final models, designated **1** to **3**, are given in Table 2. That neither *C* nor Ω is able to discriminate between them suggests that these are all equally stable models. Their atomic coordinates are given in Table 3.

The variability of side-group geometry in the arabinogalactan molecule is vividly evident from Fig. 3, which shows two mutually perpendicular views in each model. The side groups spiral around the rigid galactan core such that the cylindrical shape is conserved. However, the diameter increases from a low 29.6 Å in **2** to 31.8 Å in **1** to a high 36.6 Å in **3**. Compatible with the extent to which they stretch out, the alignment of the side groups relative to the molecular axis distinguishes one model from another: *B* and *C* turn down so that *C* is fully exposed in **1**; they are tilted up in **3**; and the situation is intermediate in **2**. On the other hand, the axial views highlight their unique fingerprints. The projections resemble those of a pinwheel, hexagon and snowflake in **1**, **2** and **3**, respectively. Interchain hydrogen bonds (O-2B···O-2C and O-3B···O-3C) are present only in **2**.

As a result of these morphological differences, the helices are packed in the hexagonal unit cell (space group $P6_3$) in quite distinct ways as shown in Fig. 4. Neighboring pinwheels of **1** are held in place by O-6C···O-4C hydrogen bonds (Fig. 4a); the hexagons of **2** are connected by O-6C···O-6C interactions (Fig. 4b); and the snowflakes of **3** are joined by O-6C···O-3B hydrogen bonds (Fig. 4c). The hexagons appear to associate more closely than the pinwheels, whereas the snowflakes interdigitate due to their fully extended side groups.

4. Discussion

This modeling analysis has demonstrated that (1→3)-β-galactan can assume the same triple-helical struc-

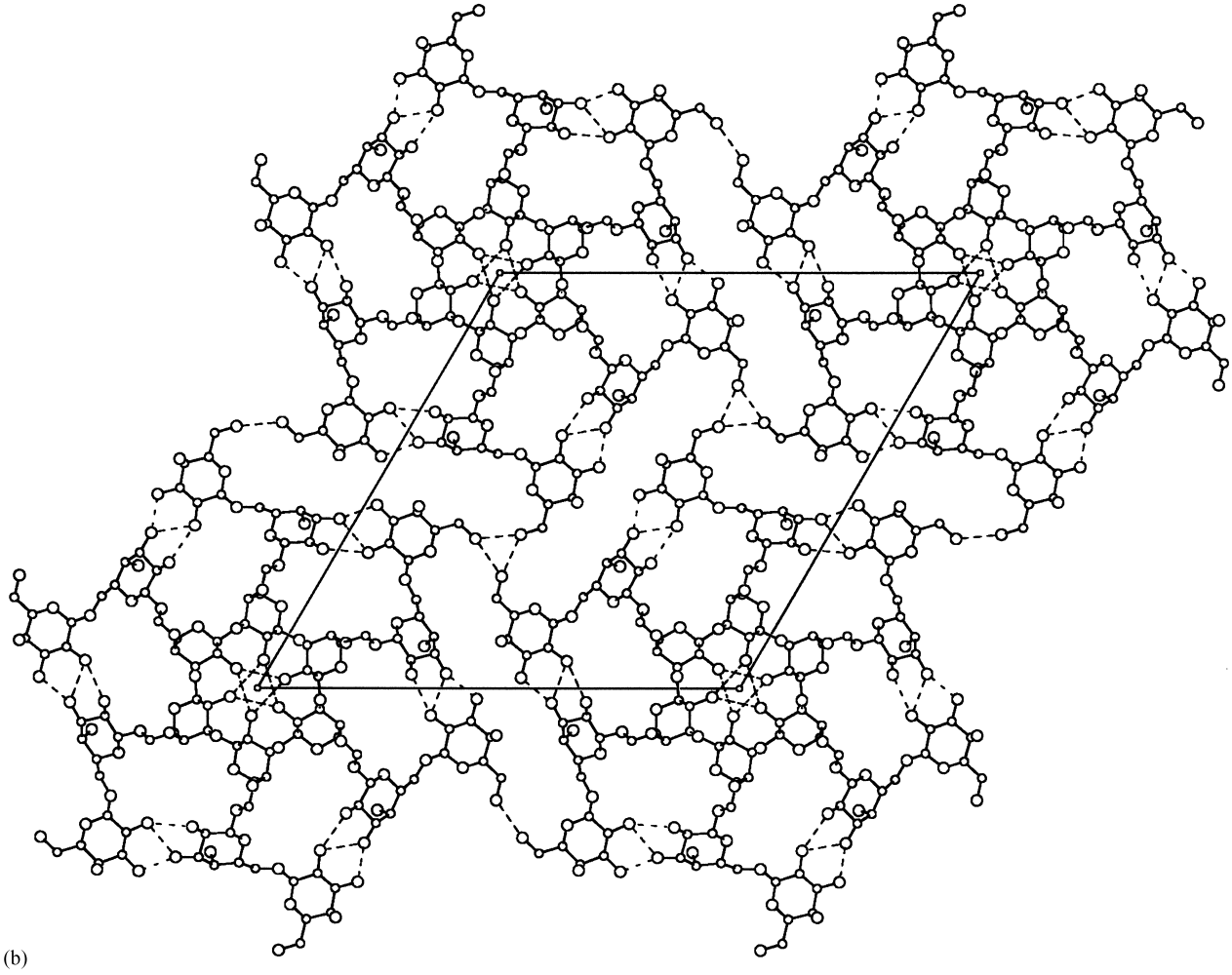

Fig. 4. (*Continued*)

ture of (1→3)-β-glucan first reported for curdlan[7] and later adopted for scleroglucan[6] (Glc side group substituted at the 6th position of every third Glc unit in the glucan chain). Our study is the first to demonstrate that the galactan triple helix can also accommodate a disaccharide Gal-(1→6)-Gal substituted at the 6th position in every Gal unit in the main chain. The side group attachment is not unique as it can be done in several ways while preserving the helix symmetry. The variety of molecular models that could be generated but not discriminated on steric grounds is clear testimony that the branched polymer, representing the prototype arabinogalactan molecule, is extremely polymorphic.

Such polymorphism in molecular structure will deter lateral organization of the polymer helices. This is the major structural reason for the lack of crystallinity leading to inferior diffraction pattern as observed in Fig. 1. While the side group distribution is uniform in our 'idealized' prototype model, this is far from true in the 'actual' arabinogalactan molecule. This departure will certainly influence not only the molecular structure but also the associative properties. For example, sites with or without substitution, or sites substituted with a monomer or a different sugar will all cause only local perturbations and not affect the overall helix geometry. On the other hand, the major impact will be on lateral organization of the helices. In any case, the side groups appear to perform dual roles in the arabinogalactan molecule that resembles a bottle brush. Firstly, like the bristles of the brush, they shield the galactan triple helix from external turbulences so that the central core stays strong. Secondly, like flexible bristles, they stretch out and sweep around so as to interact with neighboring helices via hydrogen bonds. These features are fully consistent with the expected solution behavior of arabinogalactan[15] as a hydrocolloid and not a gelling agent that would require some lateral organization or partial crystallinity.

In the ideal situation, the arabinogalactan helix should have a *c*-repeat close to 6 Å and space group $P6_3$ that mimics curdlan III.[7] However, the arabinogalactan diffraction pattern (Fig. 1) shows that *c* is 3

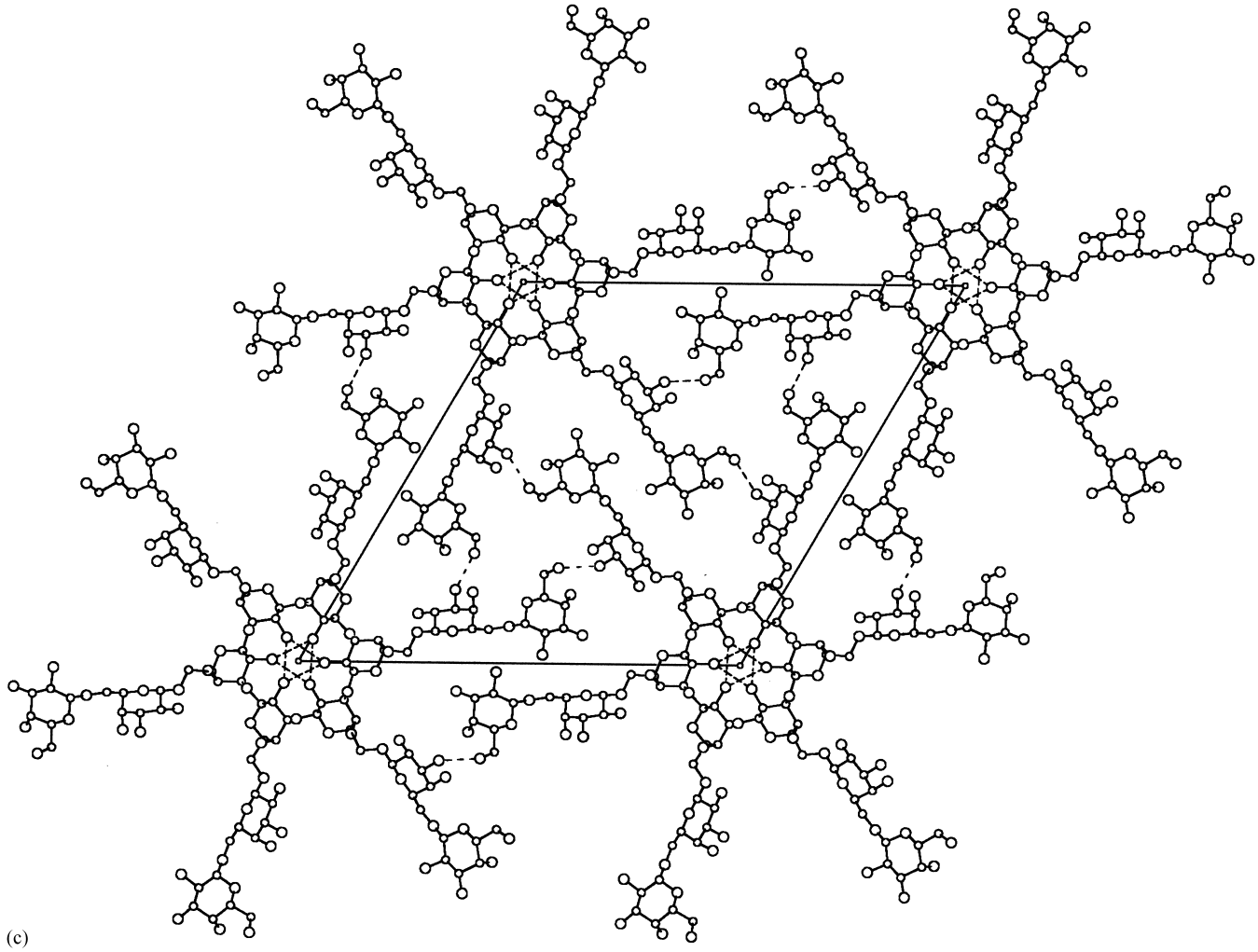

Fig. 4. (*Continued*)

times 5.9 Å, suggesting that the side groups in the helix do not have identical conformations. The larger *c*-repeat (17.7 Å) is readily explained in the light of significant conformational freedom available to the side groups (Table 1). A similar argument was used for curdlan II ($c = 18.8$ Å) in terms of a gamut of hydroxymethyl group orientations within the triple helix.[16]

A helix-forming polymer molecule composed of a rigid core decorated with a series of flexible arms having many hydroxyl groups can always be exploited as a carrier for drug delivery and related functions. The structural features emerging from our modeling analysis suggest that the arabinogalactan molecule would serve these purposes. The precise molecular details must however await better experimental data.

Acknowledgements

This research was supported by the Industrial Consortium of the Whistler Center for Carbohydrate Research. We thank Prof. Roy Whistler for sharing the arabinogalactan sample and related information.

References

1. Chandrasekaran, R. *Adv. Carbohydr. Chem. Biochem.* **1997**, *52*, 311–439.
2. Chandrasekaran, R. *Adv. Food Nutr. Res.* **1998**, *42*, 131–210.
3. Chandrasekaran, R.; Bian, W.; Okuyama, K. *Carbohydr. Res.* **1998**, *312*, 219–224.
4. Chandrasekaran, R.; Radha, A.; Lee, E. J. *Carbohydr. Res.* **1994**, *252*, 183–207.
5. Bian, W.; Chandrasekaran, R.; Rinaudo, M. *Carbohydr. Res.* **2002**, *337*, 45–56.
6. Bluhm, T. L.; Deslandes, Y.; Marchessault, R. H.; Pérez, S.; Rinaudo, M. *Carbohydr. Res.* **1982**, *100*, 117–130.
7. Deslandes, Y.; Marchessault, R. H.; Sarko, A. *Macromol.* **1980**, *13*, 1466–1471.
8. Ponder, G. R.; Richards, G. N. *Carbohydr. Polym.* **1997**, *34*, 251–261.
9. Dong, Q.; Fang, J. *Carbohydr. Res.* **2001**, *332*, 109–114.

10. Huisman, M. M. H.; Brüll, L. P.; Thomas-Oates, J. E.; Haverkamp, J.; Schols, H. A.; Voragen, A. G. J. *Carbohydr. Res.* **2001**, *330*, 103–114.
11. Loosveld, A-M. A; Grobet, P. J.; Delcour, J. A. *J. Agric. Food Chem.* **1997**, *45*, 1998–2002.
12. Tischer, C. A.; Iacomini, M.; Gorin, P. A. J. *Carbohydr. Res.* **2002**, in press.
13. Smith, P. J. C.; Arnott, S. *Acta Crystallogr.* **1978**, *A34*, 3–11.
14. Hamilton, W. C. *Acta Crystallogr.* **1965**, *18*, 502–510.
15. Whistler, R. L.; BeMiller, J. N. *Carbohydrate Chemistry for Food Scientists*; Eagan Press: Minnesota, 1997; pp 168–169.
16. Chuah, C. T.; Sarko, A.; Deslandes, Y.; Marchessault, R. H. *Macromolecules* **1983**, *16*, 1375–1382.